UT-10-12
July, 2010

Spin and Chirality Determination of Superparticles with Long-Lived Stau at the LHC

Takumi Ito[(a,b)] and Takeo Moroi[(a,c)]

[(a)] *Department of Physics, University of Tokyo, Tokyo 113-0033, JAPAN*

[(b)] *Department of Physics, Tohoku University, Sendai 980-8578, JAPAN*

[(c)] *Institute for the Physics and Mathematics of the Universe, University of Tokyo, Chiba 277-8568, Japan*

Abstract

Long-lived stau shows up in various supersymmetric models, like gauge-mediated supersymmetry (SUSY) breaking model. At the LHC experiment, long-lived stau is useful not only for the discovery of SUSY signals but also for the study of the detailed properties of superparticles. We discuss a method to obtain information on spins and chiralities of superparticles in the framework with long-lived stau. We also show that such a study can be used to distinguish SUSY model from other models of new physics, like the universal extra dimension model.

Low energy supersymmetry (SUSY) is an attractive candidate of the physics beyond the standard model, and superparticles are important targets of the LHC experiment. Even if signals of superparticles are found, however, it is non-trivial to confirm that the newly discovered particles are superparticles. This is because the SUSY-like mass spectrum is possible in some class of models other than supersymmetric one. Thus, once exotic particles are found at the LHC, their properties should be studied in detail to understand the underlying model.

Procedure to study the properties of superparticles crucially depends on their mass spectrum; in particular, for each candidate of the lightest supersymmetric particle (LSP) in the minimal supersymmetric standard model (MSSM) sector, which we call MSSM-LSP, we expect different type of SUSY signals at the LHC experiment. Even though the lightest neutralino is the most popular candidate of the MSSM-LSP, charged (and/or colored) superparticle can also be the MSSM-LSP if it is unstable. Thus, for each candidate of the MSSM-LSP, we should consider how and how well the SUSY events can be studied at the LHC.

In the present study, we consider an important possibility that the lighter stau $\tilde{\tau}$ is the MSSM-LSP. Stau can be the MSSM-LSP in well-motivated SUSY breaking scenarios, like the gauge mediated SUSY breaking scenario [1, 2]. Even though $\tilde{\tau}$ is expected to be unstable in such a case, its decay length can be much longer than the size of the LHC detectors (~ 10 m). Then, $\tilde{\tau}$ is regarded as a long-lived charged particle at the LHC experiment. For example, in the gauge-mediation model, $\tilde{\tau}$ decays into τ + gravitino, and the decay length becomes longer than 10 m if the gravitino mass is heavier than ~ 1 keV. Then, in such a case, we can observe a track of $\tilde{\tau}$ at the LHC experiment and we expect very unique signals at the LHC. The $\tilde{\tau}$ track should be useful not only for the discovery but also for the study of the properties of superparticle [3, 4, 5, 6, 7, 8, 9, 10, 11, 12, 13, 14, 15, 16, 17, 18, 19]; in particular, in the previous study, we have shown that the masses of squark, sleptons, and neutralinos can be measured with very small errors using long-lived $\tilde{\tau}$ [17].

In this letter, we extend our previous analysis to discuss how we can study the properties, in particular, spins and chiralities (i.e., handednesses), of the superparticles in the decay chain. Spin and chirality measurements for the neutralino-MSSM-LSP case have been discussed in many literatures [20, 21, 22, 23, 24, 25, 26, 27, 28]. We will see that, if $\tilde{\tau}$ is the MSSM-LSP, the study becomes easier because SUSY events can be distinguished from standard-model backgrounds by identifying $\tilde{\tau}$-track, and also because full event reconstruction is possible due to the absence of the missing momentum. Information on the particles in the decay chain is extracted from the invariant-mass distribution of the decay products. Unfortunately, the observed invariant-mass distributions are deformed from the parton-level predictions, which becomes the origin of systematic uncertainties in the test of underlying models. We propose to analyze the ratio of the numbers of two different processes with same event topology, from which many of the systematic uncertainties should cancel out. We will see that such an analysis is useful to understand the chiralities of the superpaticles in the decay chain. Furthermore, we can also distinguish SUSY model from other models with particles with different spin, like the universal extra dimension (UED) model [29], which

may result in a SUSY-like mass spectrum. We note here that, in order to make our points clear, we consider supersymmetric standard model with long-lived $\tilde{\tau}$. However, the procedure should work in other class of models, like the UED model with a long-lived Kalza-Klein (KK) charged lepton.[#1]

Let us start with discussing the underlying model we have in mind, i.e., supersymmetric model with $\tilde{\tau}$-MSSM-LSP. If low-energy SUSY exists, squarks and gluino are particularly produced at the LHC. In the following discussion, we consider the case where the gluino is heavier than squarks. (Such a mass spectrum is naturally realized, for example, in gauge mediation model with $\tilde{\tau}$-MSSM-LSP.) In such a case, the processes $pp \to \tilde{u}\tilde{u}$ and $\tilde{d}\tilde{d}$ have significant cross section compared to other processes because of large parton densities of the up- and down-quarks in proton. (Other types of SUSY processes also occur, but their effects become subdominant in the following study by imposing relevant kinematical cuts.) Then, once $\tilde{q}$ (where, here and hereafter, q is for u and d) is produced, it may cause the decay chain $\tilde{q} \to q\chi_1^0$, followed by $\chi_1^0 \to \tau^\pm \tilde{\tau}^\mp$ (with χ_1^0 being the lightest neutralino); for simplicity, we denote such a decay chain as $\tilde{q} \to q\tau^\pm\tilde{\tau}^\mp$. In the following, we only use the hadronic decay mode of τ. Then, SUSY events result in $\tilde{\tau}$ tracks and τ-jets as well as energetic jets. If the velocity of $\tilde{\tau}$ is small enough, SUSY events can be distinguished from the standard-model events by identifying $\tilde{\tau}$ track. The discovery of such events should be a clear indication of the existence of a new physics beyond the standard model. In addition, with the study of the endpoints or peak positions of the invariant-mass distributions, information on the masses of the new particles (i.e., squarks and neutralinos) will be obtained [17].

Once the masses of newly discovered particles are determined, the next task will be to precisely understand the underlying model. In particular at the early stage of the LHC experiment, it is non-trivial to confirm that the underlying model is MSSM. In the present case, the existence of particles with masses of $m_{\tilde{q}_R}$ and $m_{\chi_1^0}$ as well as a long-lived charged particle can be experimentally confirmed. However, if the masses are the only information available from the experiment, it is not clear if those particles are superparticles. In addition, even if the underlying model is assumed to be the MSSM, chiralities of observed $\tilde{q}$ and $\tilde{\tau}$ are unknown. As we have mentioned, the information on the underlying model is imprinted in the invariant-mass distributions of the particles from the decay; in order to confirm or exclude a specific underlying model, one should check the consistency between observed invariant-mass distribution and prediction of the postulated model. In the following, we discuss how and how well we can perform such an analysis.

In the present case, invariant mass of (q, τ) system contains important information. For the study of the SUSY model, we parameterize the relevant interaction terms as

$$\mathcal{L}_{\rm int} = \bar{\chi}_1^0(g_{q,L}P_L + g_{q,R}P_R)q\tilde{q}^* + \bar{\chi}_1^0(g_{\tau,L}P_L + g_{\tau,R}P_R)\tau\tilde{\tau}^* + \text{h.c.}, \tag{1}$$

where $g_{q,L}$, $g_{q,R}$, $g_{\tau,L}$, and $g_{\tau,R}$ are coupling constants. (In the following, we consider the

[#1] In the simplest UED model, KK mode of the $U(1)_Y$ is the lightest KK particle (LKP). However, such a mass spectrum can be easily modified by introducing the brane-localized interactions. Then, the long-lived KK lepton may show up when the KK mode of the graviton is the LKP while the KK mode of a lepton is the second-lightest KK particle.

case that the production of right-handed squarks plays an important role and also that the lighter stau is right-handed. Then, for the process we will study, $g_{q,L} = g_{\tau,L} = 0$.) The invariant-mass distributions of the decay processes are given by

$$\frac{1}{2\Gamma_{\tilde{q}\to q\tau^+\tilde{\tau}^-}}\frac{d\Gamma_{\tilde{q}\to q\tau^+\tilde{\tau}^-}}{dx_{q\tau}} = \frac{(g_{q,L}^2 g_{\tau,L}^2 + g_{q,R}^2 g_{\tau,R}^2)(1-x_{q\tau}) + (g_{q,L}^2 g_{\tau,R}^2 + g_{q,R}^2 g_{\tau,L}^2)x_{q\tau}}{g_{q,L}^2 g_{\tau,L}^2 + g_{q,R}^2 g_{\tau,R}^2 + g_{q,L}^2 g_{\tau,R}^2 + g_{q,R}^2 g_{\tau,L}^2}, \quad (2)$$

$$\frac{1}{2\Gamma_{\tilde{q}\to q\tau^-\tilde{\tau}^+}}\frac{d\Gamma_{\tilde{q}\to q\tau^-\tilde{\tau}^+}}{dx_{q\tau}} = \frac{(g_{q,L}^2 g_{\tau,L}^2 + g_{q,R}^2 g_{\tau,R}^2)x_{q\tau} + (g_{q,L}^2 g_{\tau,R}^2 + g_{q,R}^2 g_{\tau,L}^2)(1-x_{q\tau})}{g_{q,L}^2 g_{\tau,L}^2 + g_{q,R}^2 g_{\tau,R}^2 + g_{q,L}^2 g_{\tau,R}^2 + g_{q,R}^2 g_{\tau,L}^2}, \quad (3)$$

and $d\Gamma_{\tilde{q}^*\to q\tau^\pm\tilde{\tau}^\mp}/dx_{q\tau} = d\Gamma_{\tilde{q}\to q\tau^\mp\tilde{\tau}^\pm}/dx_{q\tau}$, where

$$x_{q\tau} = M_{q\tau}^2/\hat{M}_{q\tau}^2 = (p_q + p_\tau)^2/\hat{M}_{q\tau}^2, \quad (4)$$

with $\hat{M}_{q\tau}^2$ being the maximal value of $M_{q\tau}^2$:

$$\hat{M}_{q\tau}^2 = \frac{(m_{\tilde{q}}^2 - m_{\chi_1^0}^2)(m_{\chi_1^0}^2 - m_{\tilde{\tau}}^2)}{m_{\chi_1^0}^2}. \quad (5)$$

Because of the Majorana nature of χ_1^0, $\Gamma_{\tilde{q}\to q\tau^+\tilde{\tau}^-} = \Gamma_{\tilde{q}\to q\tau^-\tilde{\tau}^+}$. One can easily see that $d\Gamma_{\tilde{q}\to q\tau^\pm\tilde{\tau}^\mp}/dx_{q\tau}$ has non-trivial dependence on $x_{q\tau}$. We also note here that the distributions of $M_{q\tau}^2$ depend on the chiralities of $\tilde{q}$ and $\tilde{\tau}$ and that the invariant-mass distributions are different for $\tilde{q}\to q\tau^+\tilde{\tau}^-$ and $\tilde{q}\to q\tau^-\tilde{\tau}^+$. These facts are important in the following discussion. The distributions given in Eqs. (2) and (3) are crucial check points of the present model.

Now, we show how the observed invariant-mass distributions behave by using the MC analysis. In our study, we work in the framework of gauge-mediated model. We consider the situation that the MSSM-LSP is lighter stau $\tilde{\tau}$, which is assumed to be long-lived, and that the processes $pp\to\tilde{u}\tilde{u}$ and $\tilde{d}\tilde{d}$ have large cross sections. We adopt the following parameters:

$$\Lambda = 60 \text{ TeV}, \quad M_{\rm mess} = 900 \text{ TeV}, \quad N_{\mathbf{5}} = 3, \quad \tan\beta = 35, \quad \text{sign}(\mu) = +, \quad (6)$$

where Λ is the ratio of the F- and A-components of the SUSY breaking field, $M_{\rm mess}$ is the messenger scale, $N_{\mathbf{5}}$ is the number of messenger multiplets in units of $\mathbf{5}+\bar{\mathbf{5}}$ representation of $SU(5)$ grand-unified group, $\tan\beta$ is the ratio of the vacuum expectation values of two Higgs bosons, and μ is the SUSY invariant Higgs mass. The mass spectrum of superparticles is calculated by using ISAJET 7.64 [30]; the result is summarized in Table 1. The LHC phenomenology of this parameter point has been studied in [17], which has shown that the masses of superparticles can be determined with relatively small uncertainties. In particular, $m_{\tilde{q}_R}$ and $m_{\chi_1^0}$ are measured with the accuracies of ~ 10 GeV and ~ 1 GeV, respectively, with the luminosity of $\mathcal{L} = 100$ fb^{-1}. In addition, $m_{\tilde{\tau}}$ can be also determined by combining time-of-flight and momentum information; the expected accuracy is ~ 0.1 GeV [8]. In our study, we assume that the masses of these superparticles can be well determined before the study of the invariant-mass distributions.

Particle	Mass (GeV)
$\tilde{g}$	1309.39
$\tilde{u}_L$	1231.70
$\tilde{u}_R$	1183.97
$\tilde{d}_L$	1234.28
$\tilde{d}_R$	1180.19
$\tilde{t}_1$	1082.85
$\tilde{t}_2$	1195.08
$\tilde{b}_1$	1145.24
$\tilde{b}_2$	1185.83
$\tilde{\nu}_l$	388.05
$\tilde{l}_L$	396.19
$\tilde{\tau}_2$	402.57
$\tilde{\nu}_\tau$	383.80
$\tilde{l}_R$	194.39
$\tilde{\tau}_1$	148.83
χ_1^0	239.52
χ_2^0	425.92
χ_3^0	508.41
χ_4^0	548.67
$\chi_1^\pm$	425.45
$\chi_2^\pm$	548.43
h	115.01

Table 1: Masses of the superparticles and the lightest Higgs boson h in units of GeV. The input parameters are $\Lambda = 60$ TeV, $M_{\rm mess} = 900$ TeV, $N_{\mathbf{5}} = 3$, $\tan\beta = 35$, sign$(\mu) = +$. (We use the top-quark mass of 171.3 GeV.)

We have generated SUSY events for $\sqrt{s} = 14$ TeV with HERWIG 6.510 package [31, 32]. (The total cross section of the SUSY events is 669.6 fb.) In order to simulate detector effects, we use the PGS4 detector simulator [33] with slight modification to treat stable stau; the momentum resolution of $\tilde{\tau}$ is assumed to be the same as those of muons. Following [4], we assume that $\tilde{\tau}$ with $0.4 \leq \beta_{\tilde{\tau}} \leq 0.91$ can be detected with the efficiency of 100 % with no standard-model background. Staus with $\beta_{\tilde{\tau}} \geq 0.91$ are assumed to be identified as muons.

In order to use the events with the decay chain $\tilde{q} \to q\chi_1^0$, followed by $\chi_1^0 \to \tau^{\pm}\tilde{\tau}^{\mp}$, the following selection cuts are applied:

(a) At least one $\tilde{\tau}$ with the velocity $0.4 \leq \beta_{\tilde{\tau}} \leq 0.91$.

(b) At least one τ-tagged jet j_τ with $p_T > 20$ GeV.

(c) Exactly two jets j with $p_T > 30$ GeV.

The requirement (c) is to eliminate the gluino production events. If there exists only one $\tilde{\tau}$ with $0.4 \leq \beta_{\tilde{\tau}} \leq 0.91$, the highest p_T muon-like object is regarded as second $\tilde{\tau}$ because two staus are expected in SUSY events. Then, for all the possible combinations of $(j, j_\tau, \tilde{\tau})$, we perform the following study. We first reconstruct the tau momentum p_τ assuming that tau and stau are from the decay of χ_1^0 (whose mass is expected to be already known). Because the tau from the neutralino decay is highly boosted, we approximate that the three-momentum of τ is parallel to that of j_τ. Then, we obtain

$$p_\tau = z_{\tilde{q}}^{-1} p_{j_\tau}, \tag{7}$$

where

$$z_{\tilde{q}} = \frac{2 p_{j_\tau} p_{\tilde{\tau}}}{m_{\chi_1^0}^2 - m_{\tilde{\tau}}^2}. \tag{8}$$

Combinations with $z_{\tilde{q}} > 1$ is eliminated. Then, we calculate

$$M_{\tilde{q}} = \sqrt{(p_j + p_{\tilde{\tau}} + z_{\tilde{q}}^{-1} p_{j_\tau})^2}. \tag{9}$$

Using the fact that there exists a very sharp peak in the distribution of $M_{\tilde{q}}$, which is from $\tilde{q}_R$ production, only the combinations with $m_{\tilde{q}_R}^{(\mathrm{peak})} - 40$ GeV $\leq M_{\tilde{q}} \leq m_{\tilde{q}_R}^{(\mathrm{peak})} + 40$ GeV are adopted, where $m_{\tilde{q}_R}^{(\mathrm{peak})} = 1170$ GeV is the position of the peak [17].[#2] We calculate the distribution of the following variable:

$$x_{j\tau} \equiv M_{j\tau}^2 / \hat{M}_{j\tau}^2 \equiv (p_j + z_{\tilde{q}}^{-1} p_{j_\tau})^2 / \hat{M}_{j\tau}^2, \tag{10}$$

where

$$\hat{M}_{j\tau}^2 = \frac{(M_{\tilde{q}}^2 - m_{\chi_1^0}^2)(m_{\chi_1^0}^2 - m_{\tilde{\tau}}^2)}{m_{\chi_1^0}^2}. \tag{11}$$

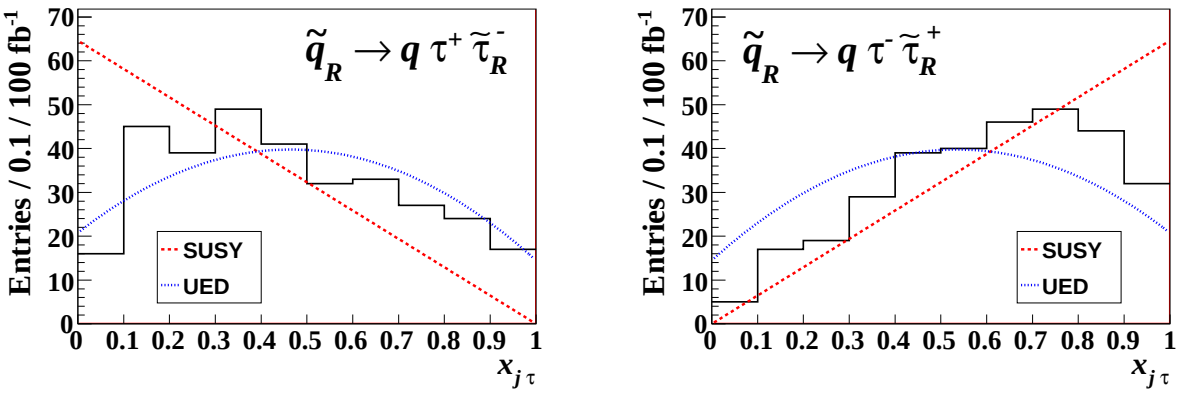

Figure 1: Distributions of $x_{j\tau}$ in the reconstructed decay processes, $\tilde{q}_R \to q\tau^+\tilde{\tau}_R^-$ (left) and $\tilde{q}_R \to q\tau^-\tilde{\tau}_R^+$ (right), where $x_{j\tau}$ is a squared invariant mass normalized by its maximal value. Here we take $\mathcal{L} = 100$ fb^{-1}. The theoretical predictions are also shown in the SUSY case (red dashed line), and for similar processes in the UED case (blue dotted line).

The charges of j_τ and $\tilde{\tau}$, which are both observable, should be opposite for signal events.

In Fig. 1, we show the distributions of $x_{j\tau} = M_{j\tau}^2/\hat{M}_{j\tau}^2$ for $(j, j_\tau^+, \tilde{\tau}^-)$ and $(j, j_\tau^-, \tilde{\tau}^+)$ events. In the same figure, we also plot the theoretical differential decay rates given in Eqs. (2) and (3); the normalization is determined so that the total number of events agrees with the MC data. The MC results and the theoretical predictions seem to agree at qualitative level.

At quantitative level, however, the agreement is not perfect. We can see that the numbers of events are suppressed when $x_{j\tau} \to 0$ and 1. These can be understood by considering the event configurations in those limits. When $x_{j\tau} \to 0$, τ is emitted in the opposite direction to χ_1^0 in the rest frame of $\tilde{q}$. Because most of the squarks are not significantly boosted with the present choice of the squark masses, τ in events with small $x_{j\tau}$ are likely to have small p_T. Because the p_T of j_τ is required to be larger than 20 GeV, the acceptance of the signal is suppressed for $x_{j\tau} \sim 0$. On the contrary, when $x_{j\tau} \to 1$, the momenta of τ and $\tilde{\tau}$ become parallel in the rest frame of $\tilde{q}$. Such events are eliminated by the isolation cut for the τ-jet; in the present analysis, no extra activity is allowed in the cone (with the size of $\Delta R = 0.5$) around τ-jet. To see the validity of these arguments, we estimate the efficiencies of corresponding kinematical cuts using the momentum information on the decay products obtained from HERWIG output. The results are shown in Tables 2 and 3. We can see that the efficiencies behave as we have expected. It is also notable that the efficiencies depend on $x_{j\tau}$, but are insensitive to the charges of final-state τ and $\tilde{\tau}$.

Another important reason of the disagreement should be the contamination of background, which can be from fake τ-jets (mis-identified QCD jets) as well as from wrong

[#2]The peak position in the present study is found to be smaller than the input value of the squark mass by ~ 10 GeV. This is expected to be due to the energy leakage in the jet reconstruction, and may be corrected once the jet energy is well calibrated.

Bin	$(j, j_\tau^+, \tilde{\tau}^-)$	$(j, j_\tau^-, \tilde{\tau}^+)$
$0 \le x_{q\tau} < 0.1$	0.09	0.13
$0.1 \le x_{q\tau} < 0.2$	0.19	0.21
$0.2 \le x_{q\tau} < 0.3$	0.24	0.24
$0.3 \le x_{q\tau} < 0.4$	0.25	0.25
$0.4 \le x_{q\tau} < 0.5$	0.25	0.26
$0.5 \le x_{q\tau} < 0.6$	0.27	0.27
$0.6 \le x_{q\tau} < 0.7$	0.27	0.26
$0.7 \le x_{q\tau} < 0.8$	0.29	0.28
$0.8 \le x_{q\tau} < 0.9$	0.28	0.28
$0.9 \le x_{q\tau} < 1.0$	0.32	0.28

Table 2: Ratio of the total number of squark-decay events and that with $p_T(j_\tau) \ge 20$ GeV.

Bin	$(j, j_\tau^+, \tilde{\tau}^-)$	$(j, j_\tau^-, \tilde{\tau}^+)$
$0 \le x_{q\tau} < 0.1$	0.97	0.98
$0.1 \le x_{q\tau} < 0.2$	0.95	0.94
$0.2 \le x_{q\tau} < 0.3$	0.88	0.87
$0.3 \le x_{q\tau} < 0.4$	0.80	0.79
$0.4 \le x_{q\tau} < 0.5$	0.72	0.71
$0.5 \le x_{q\tau} < 0.6$	0.62	0.61
$0.6 \le x_{q\tau} < 0.7$	0.49	0.50
$0.7 \le x_{q\tau} < 0.8$	0.41	0.39
$0.8 \le x_{q\tau} < 0.9$	0.29	0.29
$0.9 \le x_{q\tau} < 1.0$	0.26	0.18

Table 3: Ratio of the total number of squark-decay event and that with $\Delta R_{j_\tau \tilde{\tau}} \ge 0.5$.

combination where τ and $\tilde{\tau}$ have different parents. Once the real data will become available, an accurate determination of the number of backgrounds may be possible using, for example, events off from the squark-mass peak (i.e., the sideband). In the present MC analysis, we have estimated the shape of the background from the sideband samples, and the number of backgrounds in each bin is inferred to be approximately universal as far as $x_{j\tau}$ is not close to 0 or 1. In the following analysis, we adopt constant background in each bin. Since the accurate estimation of the total number of backgrounds is difficult from the sideband samples in the present analysis, the normalization of background is treated as a free parameter and is determined so that the χ^2 variable defined below is minimized.

If the effects of the deformation will be well understood in future by, for example, a reliable MC analysis, the invariant-mass distributions may be directly used to discriminate underlying models. However, it is desirable to find quantities which are insensitive to the effects of deformation. For this purpose, we consider the ratio of the numbers of $(j, j_\tau^+, \tilde{\tau}^-)$

and $(j, j_\tau^-, \tilde{\tau}^+)$ events; we define

$$L_i = \ln \frac{N_i(j, j_\tau^+, \tilde{\tau}^-)}{N_i(j, j_\tau^-, \tilde{\tau}^+)}, \tag{12}$$

where $N_i(j, j_\tau^\pm, \tilde{\tau}^\mp)$ are the numbers of events in i-th bin with charges of $(j_\tau, \tilde{\tau})$ being $(\pm, \mp)$. The error of L_i is given by

$$\delta L_i^2 = \frac{1}{N_i(j, j_\tau^+, \tilde{\tau}^-)} + \frac{1}{N_i(j, j_\tau^-, \tilde{\tau}^+)}. \tag{13}$$

To discuss how well the theoretical prediction is expected to agree with experimental result, we calculate

$$\chi^2 \equiv \sum_i \frac{(L_i - L_i^{(\rm th)})^2}{\delta L_i^2}, \tag{14}$$

where $L_i^{(\rm th)}$ is the theoretical prediction which is given by

$$L_i^{(\rm th)} = \ln \frac{N_i^{(\rm signal)}(j, j_\tau^+, \tilde{\tau}^-) + N^{(\rm BG)}}{N_i^{(\rm signal)}(j, j_\tau^-, \tilde{\tau}^+) + N^{(\rm BG)}}, \tag{15}$$

and the summation is over the bins in the range of $0.1 \leq x_{j\tau} \leq 0.9$ (with the width of $\Delta x_{j\tau} = 0.1$); in order to minimize the effects of background contamination, we do not use the bins at $x_{j\tau} \sim 0$ and 1. Here, $N_i^{(\rm signal)}(j, j_\tau^\pm, \tilde{\tau}^\mp)$ are theoretical predictions of the number of signal events in i-th bin calculated from Eqs. (2) and (3), while $N^{(\rm BG)}$ is the number of background events in each bin, which is independent of i.

L_i from the MC analysis is shown in Fig. 2 for $\mathcal{L} = 100$ fb^{-1}. In the same figure, theoretical predictions $L_i^{(\rm th)}$ are also shown. We can see that the MC result well agrees with theoretical prediction of the present SUSY model. In addition, in Table 4, we show the result for an ideal case where the luminosity is sufficiently large. (Here, we generate the event for $\mathcal{L} = 20$ ab^{-1}.) The results in the table indicate that the effects of the deformation of the invariant-mass distribution almost cancel out by taking the ratio.

The value of χ^2 varies as we take different sets of event samples. In order to estimate the typical value of χ^2, we calculate χ^2 for 20 sets of MC samples (for a fixed value of luminosity $\mathcal{L}$), and obtain averaged value of χ^2. For $\mathcal{L} = 30$ and 100 fb^{-1}, the averaged values are found to be $\langle\chi^2\rangle = 7.6$ and 8.0, respectively, which indicates a good agreement between the theoretical prediction and observation. If we flip the chirality of one of $\tilde{q}$ or $\tilde{\tau}$, then the value of χ^2 significantly increases; we obtain $\langle\chi^2\rangle = 15.8$ and 31.5 for $\mathcal{L} = 30$ and 100 fb^{-1}, respectively. This provides important information on the particles in the decay chain; the result indicates that the squarks in the observed peak and the lighter stau have the same chirality rather than different ones. Information on the chirality of $\tilde{\tau}$ may be obtained from other observables; one of the examples is the tau polarization [19]. Then, assuming SUSY

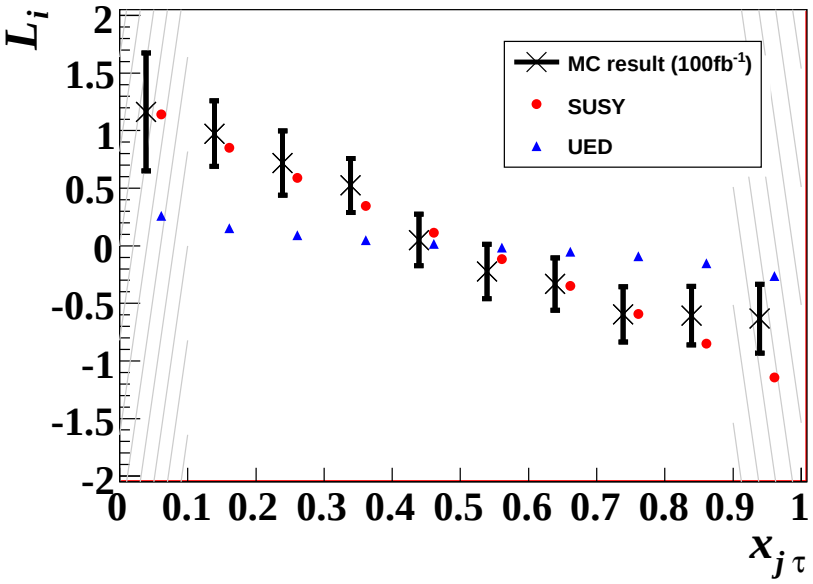

Figure 2: Distribution of L_i. MC result for $\mathcal{L} = 100$ fb^{-1} is cross with error bar. Theoretical predictions of L_i obtained after minimizing χ^2 are also shown for the SUSY case (red circles), and the UED case (blue triangles).

model as the underlying model, we obtain information on the chirality of the dominantly produced squarks.

Once the data from the SUSY events are collected in the LHC experiment, we can also exclude class of models other than SUSY model by studying the distribution of the invariant mass of (q, τ) system. For a model-independent analysis, we parameterize the distribution of $x_{q\tau}$ for the decay chain resulting in $\tau^{\pm}$ (and opposite-charge long-lived particle) as

$$\frac{1}{\Gamma_{q\tau^{\pm}}}\frac{d\Gamma_{q\tau^{\pm}}}{dx_{q\tau}} = \frac{6}{c_2+6}\left[1 \pm c_1\left(2x_{q\tau}-1\right) + c_2 x_{q\tau}(1-x_{q\tau})\right], \tag{16}$$

where c_1 and c_2 are constants (with $|c_1| \leq 1$ and $c_2 \geq 0$). In the present SUSY model, $(c_1^{(\mathrm{SUSY})}, c_2^{(\mathrm{SUSY})}) = (-1, 0)$. If the underlying model is assumed to be the UED model, we would identify the particles with the masses of $m_{\tilde{q}_R}$ and $m_{\chi_1^0}$ with KK modes of q (denoted as $q^{(\mathrm{KK})}$) and neutral gauge boson (denoted as $B_\mu^{(\mathrm{KK})}$), respectively, as well as the long-lived charged particle with the KK mode of τ (denoted as $\tau^{(\mathrm{KK})}$). In this framework, there exists a similar decay chain as in the present SUSY model (i.e., $q^{(\mathrm{KK})} \to q B_\mu^{(\mathrm{KK})}$, followed by

Bin	L_i	$\delta L_i^{(100)}$	$L_i^{(\mathrm{th,SUSY})}$	$L_i^{(\mathrm{th,UED})}$
$0 \le x_{j\tau} < 0.1$	0.97	0.45	0.91	0.26
$0.1 \le x_{j\tau} < 0.2$	0.72	0.30	0.69	0.15
$0.2 \le x_{j\tau} < 0.3$	0.50	0.27	0.48	0.09
$0.3 \le x_{j\tau} < 0.4$	0.29	0.25	0.29	0.05
$0.4 \le x_{j\tau} < 0.5$	0.07	0.24	0.09	0.02
$0.5 \le x_{j\tau} < 0.6$	-0.12	0.24	-0.09	-0.02
$0.6 \le x_{j\tau} < 0.7$	-0.31	0.24	-0.29	-0.05
$0.7 \le x_{j\tau} < 0.8$	-0.47	0.25	-0.48	-0.09
$0.8 \le x_{j\tau} < 0.9$	-0.65	0.26	-0.69	-0.15
$0.9 \le x_{j\tau} < 1.0$	-0.86	0.32	-0.91	-0.26

Table 4: L_i, $\delta L_i^{(100)}$ (which is the error for the case of $\mathcal{L} = 100$ fb^{-1}), and $L_i^{(\mathrm{th})}$ for the case of large enough luminosity. The error of L_i for the luminosity $\mathcal{L}$ is given by $\delta L_i = \delta L_i^{(100)}/\sqrt{\mathcal{L}_{100}}$ with $\mathcal{L}_{100}$ being the luminosity in units of 100 fb^{-1}.

$B_\mu^{(\mathrm{KK})} \to \tau\tau^{(\mathrm{KK})}$). Then, we obtain

$$c_1^{(\mathrm{UED})} = -\epsilon_q^{(\mathrm{UED})}\epsilon_\tau^{(\mathrm{UED})}\frac{2m_{\chi_1^0}^4}{m_{\tilde{q}_R}^2 m_{\tilde{\tau}}^2 + 2m_{\chi_1^0}^4}, \tag{17}$$

$$c_2^{(\mathrm{UED})} = \frac{4m_{\chi_1^0}^2 \hat{M}_{q\tau}^2}{m_{\tilde{q}_R}^2 m_{\tilde{\tau}}^2 + 2m_{\chi_1^0}^4}, \tag{18}$$

where $\epsilon_f^{(\mathrm{UED})} = +1$ when the fermion f is right-handed (i.e., singlet under $SU(2)_L$) while $\epsilon_f^{(\mathrm{UED})} = -1$ when f is left-handed. One can see that the distribution is different from the SUSY case; this is due to the fact that the distribution depends on the spins of particles in the decay chain. Using the mass spectrum of the present model, $(c_1^{(\mathrm{UED})}, c_2^{(\mathrm{UED})}) \simeq (-0.17, 5.0)$ or $(0.17, 5.0)$, depending on the relative chirality of the KK modes of q and τ. (For comparison, we also show the results for the UED case in Figs. 1 and 2, and Table 4 for the case $(c_1^{(\mathrm{UED})}, c_2^{(\mathrm{UED})}) \simeq (-0.17, 5.0)$, which results in a smaller value of χ^2.) Furthermore, in a model where the invariant-mass distribution is flat in the phase space, $(c_1^{(\mathrm{flat})}, c_2^{(\mathrm{flat})}) = (0, 0)$. In Fig. 3, we show the contours of $\langle\chi^2\rangle = 14.1$, which correspond to 95 % C.L. bounds for 7 degrees of freedom. In the same figure, we also show the points corresponding to various models. We can see that the analysis based on the ratio of the numbers of $(j, j_\tau^+, \tilde{\tau}^-)$ and $(j, j_\tau^-, \tilde{\tau}^+)$ events is useful for the test of underlying models. We note here that, on the contours given in Fig. 3, N_{BG} is estimated to be smaller than the number of signal events in average. Thus, in the present case, constraint on c_1 vs. c_2 plane can be obtained without knowing the maximal possible number of backgrounds in detail; this is because L_i is strongly dependent on $x_{j\tau}$, as shown in Table 4, in the sample point used in our analysis. In the case with an underlying model giving rise to a weaker $x_{j\tau}$-dependence of L_i, careful estimation of the maximal number of backgrounds may be necessary to discriminate underlying models.

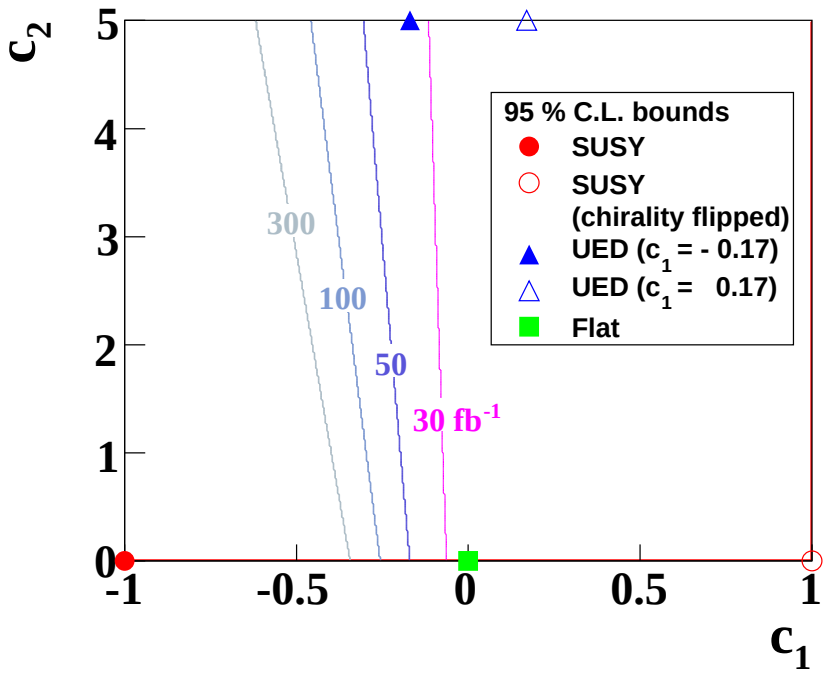

Figure 3: 95 % C.L. bounds on the c_1 vs. c_2 plane for integrated luminosities indicated in the figure. The region right to the contour is excluded for each luminosity.

In this letter, we have considered a procedure to study the properties of superparticles in the case where the lighter stau is long-lived. We have shown that properties of the particles in the decay chain are extracted from invariant-mass distributions of the decay products of $\tilde{q}$. In particular, we emphasize that the effects of the deformation of the invariant-mass distributions are largely reduced by taking the ratio of two different decay processes with the same event topology, which are, in the present case, $\tilde{q} \to q\chi_1^0$, followed by $\chi_1^0 \to \tau^+\tilde{\tau}^-$ and by $\chi_1^0 \to \tau^-\tilde{\tau}^+$. We also note here that, in some of the model beyond the standard model, a number of particles (like neutralinos) decay into two different final states which are charge-conjugated to each other, and that the reduction of the effects of deformation by taking the ratio may be useful in various cases even if there is no long-lived heavy charged particle.

In the present study, we have assumed that the squark(s) responsible for the peak in the $M_{\tilde{q}}$ distribution has unique chirality. This should be also experimentally confirmed. One of the circumstantial evidences of this may be negative observation of the decay processes of squarks into Wino-like chargino and neutralino (because the squarks are right-handed). In addition, it may be also possible to reconstruct $\tilde{q}_L$ production event to determine the mass of the left-handed squarks, from which the observed peak in the $M_{\tilde{q}}$ distribution may be understood to be from $\tilde{q}_R$ production. These will be discussed elsewhere [34].

Acknowledgments: The authors are grateful to R. Kitano for collaboration at an early stage

of this work. They also thank M. Kakizaki for useful discussion. This work was supported in part by the Grant-in-Aid for Scientific Research from the Ministry of Education, Science, Sports, and Culture of Japan, Nos. 22540263 and 22244021 (T.M.).

References

[1] M. Dine, A. E. Nelson, Y. Nir and Y. Shirman, Phys. Rev. D **53**, 2658 (1996).

[2] M. Dine, A. E. Nelson and Y. Shirman, Phys. Rev. D **51**, 1362 (1995).

[3] I. Hinchliffe and F. E. Paige, Phys. Rev. D **60**, 095002 (1999).

[4] S. Ambrosanio, B. Mele, S. Petrarca, G. Polesello and A. Rimoldi, JHEP **0101**, 014 (2001)

[5] K. Hamaguchi, Y. Kuno, T. Nakaya and M. M. Nojiri, Phys. Rev. D **70**, 115007 (2004).

[6] J. L. Feng and B. T. Smith, Phys. Rev. D **71**, 015004 (2005) [Erratum-ibid. D **71**, 019904 (2005)].

[7] W. Buchmuller, K. Hamaguchi, M. Ratz and T. Yanagida, Phys. Lett. B **588**, 90 (2004).

[8] J. R. Ellis, A. R. Raklev and O. K. Oye, JHEP **0610**, 061 (2006).

[9] M. Ibe and R. Kitano, JHEP **0708**, 016 (2007).

[10] A. Rajaraman and B. T. Smith, Phys. Rev. D **76**, 115004 (2007).

[11] K. Ishiwata, T. Ito and T. Moroi, Phys. Lett. B **669**, 28 (2008).

[12] S. Kaneko, J. Sato, T. Shimomura, O. Vives and M. Yamanaka, Phys. Rev. D **78**, 116013 (2008)

[13] R. Kitano, JHEP **0811**, 045 (2008).

[14] S. Asai, K. Hamaguchi and S. Shirai, Phys. Rev. Lett. **103**, 141803 (2009).

[15] J. L. Feng, S. T. French, C. G. Lester, Y. Nir and Y. Shadmi, arXiv:0906.4215 [hep-ph]; J. L. Feng *et al.*, arXiv:0910.1618 [hep-ph].

[16] S. Biswas and B. Mukhopadhyaya, Phys. Rev. D **79**, 115009 (2009).

[17] T. Ito, R. Kitano and T. Moroi, JHEP **1004**, 017 (2010).

[18] S. Biswas and B. Mukhopadhyaya, Phys. Rev. D **81**, 015003 (2010).

[19] R. Kitano and M. Nakamura, arXiv:1006.2904 [hep-ph].

[20] A. J. Barr, Phys. Lett. B **596**, 205 (2004).

[21] J. M. Smillie and B. R. Webber, JHEP **0510**, 069 (2005).

[22] A. Datta, K. Kong and K. T. Matchev, Phys. Rev. D **72**, 096006 (2005) [Erratum-ibid. D **72**, 119901 (2005)].

[23] S. Y. Choi, K. Hagiwara, Y. G. Kim, K. Mawatari and P. M. Zerwas, Phys. Lett. B **648**, 207 (2007).

[24] L. T. Wang and I. Yavin, JHEP **0704**, 032 (2007).

[25] A. Alves and O. Eboli, Phys. Rev. D **75**, 115013 (2007).

[26] C. Csaki, J. Heinonen and M. Perelstein, JHEP **0710**, 107 (2007).

[27] G. L. Kane, A. A. Petrov, J. Shao and L. T. Wang, J. Phys. G **37**, 045004 (2010).

[28] W. Ehrenfeld, A. Freitas, A. Landwehr and D. Wyler, JHEP **0907**, 056 (2009).

[29] T. Appelquist, H. C. Cheng and B. A. Dobrescu, Phys. Rev. D **64**, 035002 (2001).

[30] F. E. Paige, S. D. Protopopescu, H. Baer and X. Tata, arXiv:hep-ph/0312045.

[31] G. Corcella *et al.*, JHEP **0101**, 010 (2001); arXiv:hep-ph/0210213.

[32] S. Moretti, K. Odagiri, P. Richardson, M. H. Seymour and B. R. Webber, JHEP **0204**, 028 (2002).

[33] For information on Pretty Good Simulation of high energy collisions (PGS4), see `http://www.physics.ucdavis.edu/%7Econway/research/research.html`.

[34] T. Ito, in preparation.